Bayesian reconstruction of color images acquired with a single CCD

Miguel Vega*[1], Rafael Molina[2], and Aggelos K. Katsaggelos[3]

[1] Dpto. de Lenguajes y Sistemas Informáticos,
Universidad de Granada, Granada 18071, SPAIN,
[2] Dpto. de Ciencias de la Computación e Inteligencia Artificial,
Universidad de Granada, Granada 18071, SPAIN,
[3] Department of Electrical and Computer Engineering,
Northwestern University, Evanston, IL 60208, USA

Abstract. Most of the available digital color cameras use a single Coupled Charge Device (*CCD*) with a Color Filter Array (*CFA*) in acquiring an image. In order to produce a visible color image a demosaicing process must be applied, which produces undesirable artifacts. This paper addresses the demosaicing problem from a superresolution point of view. Utilizing the Bayesian paradigm, an estimate of the reconstructed images and the model parameters is generated.

1 Introduction

Most of the available digital color cameras use a single Coupled Charge Device (*CCD*) with a Color Filter Array (*CFA*) to obtain color images. Unfortunately the color filter generates different spectral responses at every CCD cell. The most widely used CFA is the Bayer one [1]. It imposes a spatial pattern of two G cells, one R, and one B cell, as shown in Fig. 1.

Bayer camera pixels convey incomplete color information which needs to be extended to produce a visible color image. Such color processing is known as demosaicing (or de-mosaicking). From the pioneering work of Bayer [1] to nowadays a lot of attention has been paid to the demosaicing topic (see [2] for a review). The use of a CFA, and the corresponding demosaicing process produce undesirable artifacts, such as color fringe, that are difficult to avoid.

Over the last two decades research has been devoted to the problem of reconstructing a high-resolution image from multiple undersampled, shifted, degraded frames with subpixel displacement errors (see [3] for a recent review). In our previous work [4][5] we addressed the high resolution problem from complete and also from incomplete observations within the general framework of frequency domain multi-channel signal processing developed in [6]. In this paper we formulate the demosaicing problem as a high resolution problem from incomplete

* This work has been supported by the "Comisión Nacional de Ciencia y Tecnología" under contract TIC2003-00880.

observations and therefore we propose a new way to looking at the problem of demosaicing.

The rest of the paper is organized as follows. The problem formulation is described in section 2. In section 3 we describe the process for reconstructing each band of the color image and then examine how to iteratively estimate the high resolution color image. Experimental results are described in section 4. Finally, section 5 concludes the paper.

2 Problem formulation

Consider a Bayer camera with a Color Filter Array (CFA) over one CCD with $M_1 \times M_2$ pixels, as shown in Fig. 1(a). Assuming that the camera has three $M_1 \times M_2$ CCDs (as is usually the case), one for each R, G, B channels, the observed image is given by

$$\mathbf{g} = \left(\mathbf{g}^{R\,t}, \mathbf{g}^{G\,t}, \mathbf{g}^{B\,t}\right)^t \,, \tag{1}$$

where ^{t} denotes the transpose of a vector or a matrix and each one of the $M_1 \times M_2$ column vectors $\mathbf{g}^c$, $c \in \{R, G, B\}$, results from the lexicographic ordering of the two-dimensional signal in the R, G and B channels, respectively.

Due to the presence of the CFA we do not observe $\mathbf{g}$ but an *incomplete* subset of it, as shown in Fig. 1(b). Let us characterize these observed values in the Bayer camera. Let $N_1 = M_1/2$ and $N_2 = M_2/2$; then the 1-D downsampling matrices

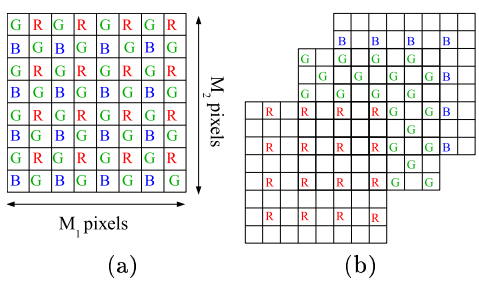

Fig. 1. (a) Pattern of channel observations for a Bayer camera with CFA; (b) Observed low resolution channels (the array in (a) and all the arrays in (b) are of the same size).

$\mathbf{D}_l^x$ and $\mathbf{D}_l^y$ are defined by

$$\mathbf{D}_l^x = \mathbf{I}_{N_1} \otimes \mathbf{e}_l^t \,, \quad \mathbf{D}_l^y = \mathbf{I}_{N_2} \otimes \mathbf{e}_l^t \,, \tag{2}$$

where $\mathbf{I}_{N_i}$ is the $N_i \times N_i$ identity matrix, $\mathbf{e}_l$ is the 2×1 unit vector whose nonzero element is in the $l-th$ position, $l \in \{0, 1\}$ and $\otimes$ denotes the Kronecker product operator. The $(N_1 \times N_2) \times (M_1 \times M_2)$ 2D downsampling matrix is now given by $\mathbf{D}_{l1,l2} = \mathbf{D}_{l1}^x \otimes \mathbf{D}_{l2}^y$, with $l1, l2 \in \{0, 1\}$.

Using the above downsampling matrices, the subimage of $\mathbf{g}$ which has been observed, $\mathbf{g}^{\text{obs}}$, may be viewed as the incomplete set of $N_1 \times N_2$ low resolution images

$$\mathbf{g}^{\text{obs}} = \left(\mathbf{g}_{1,1}^{R\,t}, \mathbf{g}_{1,0}^{G\,t}, \mathbf{g}_{0,1}^{G\,t}, \mathbf{g}_{0,0}^{B\,t}\right)^t , \tag{3}$$

where

$$\mathbf{g}_{1,1}^R = \mathbf{D}_{1,1}\mathbf{g}^R, \;\; \mathbf{g}_{1,0}^G = \mathbf{D}_{1,0}\mathbf{g}^G, \;\; \mathbf{g}_{0,1}^G = \mathbf{D}_{0,1}\mathbf{g}^G, \;\; \mathbf{g}_{0,0}^B = \mathbf{D}_{0,0}\mathbf{g}^B. \tag{4}$$

As an example Fig. 2 illustrates how $\mathbf{g}_{1,1}^R$ is obtained. Note that the origin of coordinates is located in the bottom-left side of the array. We have one observed $N_1 \times N_2$ low resolution image at R, two at G and one at B channels.

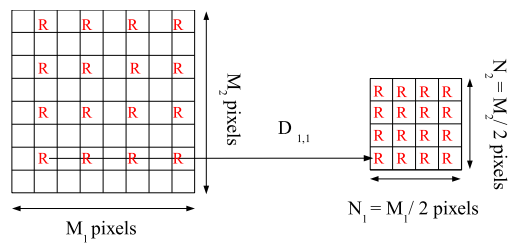

Fig. 2. Process to obtain the low resolution observed R channel

We now assume that $\mathbf{g}$ in equation (1) can be written as

$$\mathbf{g} = \begin{pmatrix} \mathbf{g}^R \\ \mathbf{g}^G \\ \mathbf{g}^B \end{pmatrix} = \begin{pmatrix} \mathbf{f}^R \\ \mathbf{f}^G \\ \mathbf{f}^B \end{pmatrix} + \begin{pmatrix} \mathbf{n}^R \\ \mathbf{n}^G \\ \mathbf{n}^B \end{pmatrix} = \mathbf{f} + \mathbf{n} \tag{5}$$

where $\mathbf{f}$ denotes the real high resolution color image we are trying to estimate and $\mathbf{n}$ denotes white independent uncorrelated noise between and within channels with variance $1/\beta^c$ in channel $c \in \{R, G, B\}$. Substituting this equation in equation (4) we have that the discrete low-resolution observed images can be written as

$$\begin{aligned} \mathbf{g}_{1,1}^R &= \mathbf{D}_{1,1}\mathbf{f}^R + \mathbf{D}_{1,1}\mathbf{n}^R, \quad & \mathbf{g}_{1,0}^G &= \mathbf{D}_{1,0}\mathbf{f}^G + \mathbf{D}_{1,0}\mathbf{n}^G, \\ \mathbf{g}_{0,1}^G &= \mathbf{D}_{0,1}\mathbf{f}^G + \mathbf{D}_{0,1}\mathbf{n}^G, \quad & \mathbf{g}_{0,0}^B &= \mathbf{D}_{0,0}\mathbf{f}^B + \mathbf{D}_{0,0}\mathbf{n}^R, \end{aligned} \tag{6}$$

where we have the following distributions for the subsampled noise

$$\begin{aligned} \mathbf{D}_{1,1}\mathbf{n}^R &\sim N(0, 1/\beta^R I_{N_1 \times N_2}), \quad & \mathbf{D}_{1,0}\mathbf{n}^G &\sim N(0, 1/\beta^G I_{N_1 \times N_2}), \\ \mathbf{D}_{0,1}\mathbf{n}^G &\sim N(0, 1/\beta^G I_{N_1 \times N_2}), \quad & \mathbf{D}_{0,0}\mathbf{n}^B &\sim N(0, 1/\beta^B I_{N_1 \times N_2}). \end{aligned} \tag{7}$$

From the above formulation, our goal has become the reconstruction of a complete RGB $M_1 \times M_2$ high resolution image $\mathbf{f}$ from the incomplete set of

observations, $\mathbf{g}^{\text{obs}}$ in equation (3). In other words, the demosaicing problem has taken the form now of a superresolution reconstruction one. We can therefore apply the theory developed in [5, 7], but taking into account that we are dealing with multichannel images and that the relationship between channels should also be taken into account [8].

3 Bayesian Reconstruction of the color image

Let us consider first the reconstruction of channel c assuming that the observed data $\mathbf{g}^{\text{obs}\,c}$ and also the real images $\mathbf{f}^{c'}$ and $\mathbf{f}^{c''}$, with $c' \neq c$ and $c'' \neq c$, are available.

In order to apply the Bayesian paradigm to this problem we define $p_c(\mathbf{f}^c)$, $p_c(\mathbf{f}^{c'}|\mathbf{f}^c)$, $p_c(\mathbf{f}^{c''}|\mathbf{f}^c)$, and $p_c(\mathbf{g}^{\text{obs}\,c}|\mathbf{f}^c)$ and use the global distribution

$$p_c(\mathbf{f}^c, \mathbf{f}^{c'}, \mathbf{f}^{c''}, \mathbf{g}^{\text{obs}\,c}) = p_c(\mathbf{f}^c) p_c(\mathbf{f}^{c'}|\mathbf{f}^c) p_c(\mathbf{f}^{c''}|\mathbf{f}^c) p_c(\mathbf{g}^{\text{obs}\,c}|\mathbf{f}^c)\,. \tag{8}$$

Smoothness within channel c is modelled by the introduction of the following prior distribution for $\mathbf{f}^c$

$$p(\mathbf{f}^c|\alpha^c) \propto (\alpha^c)^{M_1 \times M_2/2} \exp\left[-\frac{1}{2}\alpha^c \parallel \mathbf{C}\mathbf{f}^c \parallel^2\right]\,, \tag{9}$$

where $\alpha^c > 0$ and $\mathbf{C}$ denotes the Laplacian operator.

To define $p_c(\mathbf{f}^{c'}|\mathbf{f}^c)$ and similarly $p_c(\mathbf{f}^{c''}|\mathbf{f}^c)$, we proceed as follows. A two-level bank of undecimated separable two-dimensional filters constructed from a low-pass filter H_l (with impulse response $h_l = [1\ 2\ 1]/4$) and a high-pass filter H_h ($h_h = [1\ {-2}\ 1]/4$) is applied to $\mathbf{f}^{c'} - \mathbf{f}^c$ obtaining the approximation subband $W_{ll}(\mathbf{f}^{c'} - \mathbf{f}^c)$, and the horizontal $W_{lh}(\mathbf{f}^{c'} - \mathbf{f}^c)$, vertical $W_{hl}(\mathbf{f}^{c'} - \mathbf{f}^c)$ and diagonal $W_{hh}(\mathbf{f}^{c'} - \mathbf{f}^c)$ detail subbands [9] (see Fig. 3); where

$$W_{uv} = H_u \otimes H_v\,, \text{ for } uv \in \{ll, lh, hl, hh\}\,. \tag{10}$$

With this decomposition differences between channels, for high frequency components, are penalized by the introduction of the following probability distribution

$$p_c(\mathbf{f}^{c'}|\mathbf{f}^c, \gamma^{cc'}) \propto |A(\gamma^{cc'})|^{-1/2} \exp\left[-\frac{1}{2}\sum_{uv \in \mathcal{HB}} \gamma_{uv}^{cc'} \|W_{uv}(\mathbf{f}^{c'} - \mathbf{f}^c)\|^2\right]\,, \tag{11}$$

where $\mathcal{HB} = \{lh, hl, hh\}$, $\gamma_{uv}^{cc'}$ measures the similarity of the uv band of the c and c' channels, $\gamma^{cc'} = \{\gamma_{uv}^{cc'} | uv \in \mathcal{HB}\}$, and

$$A(\gamma^{cc'}) = \sum_{uv \in \mathcal{HB}} \gamma_{uv}^{cc'} W_{uv}^t W_{uv}\,. \tag{12}$$

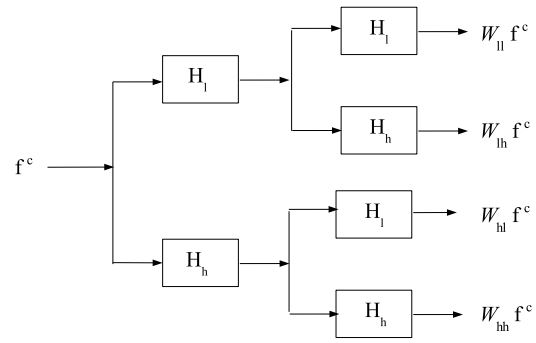

Fig. 3. Two-level filter bank

From the model in Eq. (6), we have

$$\mathrm{p}_c(\mathbf{g}^{\mathrm{obs}\,c}|\mathbf{f}^c,\beta^c) \propto \begin{cases} \beta^{R\,N_1\times N_2/2}\ \exp\left[-\frac{\beta^R}{2}\parallel \mathbf{g}^R_{1,1}-\mathbf{D}_{1,1}\mathbf{f}^R\parallel^2\right] & \text{if } c=R \\ \beta^{G\,N_1\times N_2}\ \exp\left[-\frac{\beta^G}{2}\left(\parallel \mathbf{g}^G_{1,0}-\mathbf{D}_{1,0}\mathbf{f}^G\parallel^2 + \right.\right. & \\ \qquad\qquad \left.\left.\parallel \mathbf{g}^G_{0,1}-\mathbf{D}_{0,1}\mathbf{f}^G\parallel^2\right)\right] & \text{if } c=G \\ \beta^{B\,N_1\times N_2/2}\ \exp\left[-\frac{\beta^B}{2}\parallel \mathbf{g}^B_{0,0}-\mathbf{D}_{0,0}\mathbf{f}^B\parallel^2\right] & \text{if } c=B \end{cases} \tag{13}$$

Note that from the above definitions of the probability density functions, the distribution in equation (8) depends on a set of unknown parameters and has to be properly written as

$$p_c(\mathbf{f}^c,\mathbf{f}^{c'},\mathbf{f}^{c''},\mathbf{g}^{\mathrm{obs}\,c}|\Theta^c) \tag{14}$$

where

$$\Theta^c = (\alpha_c,\gamma^{cc'},\gamma^{cc''},\beta^c)\,. \tag{15}$$

Having defined the involved distributions and the unknown parameters, the Bayesian analysis is performed to estimate the parameter vector Θ^c and the unknown high resolution band $\mathbf{f}^c$. It is important to remember that we are assuming that $\mathbf{f}^{c'}$ and $\mathbf{f}^{c''}$ are known.

The process to estimate Θ^c and $\mathbf{f}^c$ is described by the following algorithm which corresponds to the so called *evidence analysis* within the Bayesian paradigm [10].

Algorithm 1 *(*Estimation of Θ^c and $\mathbf{f}^c$ assuming that $\mathbf{f}^{c'}$ and $\mathbf{f}^{c''}$ are known*)*

Given $\mathbf{f}^{c'}$ *and* $\mathbf{f}^{c''}$

1. *Find*

$$\hat{\Theta}^c(\mathbf{f}^{c'},\mathbf{f}^{c''}) = \arg\max_{\Theta^c} p_c(\mathbf{f}^{c'},\mathbf{f}^{c''},\mathbf{g}^{obs\,c}|\Theta^c) \tag{16}$$

$$= \arg\max_{\Theta^c} \int_{\mathbf{f}^c} p_c(\mathbf{f}^c,\mathbf{f}^{c'},\mathbf{f}^{c''},\mathbf{g}^{obs\,c}|\Theta^c)d\mathbf{f}^c \tag{17}$$

2. *Find an estimate of channel c using*

$$\hat{\mathbf{f}}^c(\hat{\Theta}^c(\mathbf{f}^{c'},\mathbf{f}^{c''})) = \arg\max_{\mathbf{f}^c} p_c(\mathbf{f}^c|\mathbf{f}^{c'},\mathbf{f}^{c''},\mathbf{g}^{obs\,c},\hat{\Theta}^c(\mathbf{f}^{c'},\mathbf{f}^{c''})) \tag{18}$$

Let us now assume that we have initial estimates of the three channels, $\mathbf{f}^R(0)$, $\mathbf{f}^G(0)$ and $\mathbf{f}^B(0)$; then we can improve the quality of the reconstruction by using the following procedure

Algorithm 2 *(*Reconstruction of the color image*)*

1. *Given* $\mathbf{f}^R(0)$, $\mathbf{f}^G(0)$ *and* $\mathbf{f}^B(0)$, *initial estimates of the bands of the color image and* $\Theta^R(0)$, $\Theta^G(0)$ *and* $\Theta^B(0)$ *of the model parameters*
2. *Set k=0*
3. *Calculate*
$$\mathbf{f}^R(k+1) = \hat{\mathbf{f}}^R(\hat{\Theta}^R(\mathbf{f}^G(k),\mathbf{f}^B(k))) \tag{19}$$
by running Algorithm 1 on channel R with $\mathbf{f}^G = \mathbf{f}^G(k)$ *and* $\mathbf{f}^B = \mathbf{f}^B(k)$
4. *Calculate*
$$\mathbf{f}^G(k+1) = \hat{\mathbf{f}}^G(\hat{\Theta}^G(\mathbf{f}^R(k+1),\mathbf{f}^B(k))) \tag{20}$$
by running Algorithm 1 on channel G with $\mathbf{f}^R = \mathbf{f}^R(k+1)$ *and* $\mathbf{f}^B = \mathbf{f}^B(k)$
5. *Calculate*
$$\mathbf{f}^B(k+1) = \hat{\mathbf{f}}^B(\hat{\Theta}^B(\mathbf{f}^R(k+1),\mathbf{f}^G(k+1))) \tag{21}$$
by running Algorithm 1 on channel B with $\mathbf{f}^R = \mathbf{f}^R(k+1)$ *and* $\mathbf{f}^G = \mathbf{f}^G(k+1)$
6. *Set k=k+1 and go to step 3 until a convergence criterion is met.*

4 Experimental Results

A number of simulations have been performed with the proposed algorithm. Figure 4 shows a subset of images of size 256×384, taken from [11], used in the experiments. These images where sampled applying a Bayer pattern to get the observed images that are to be reconstructed.

The proposed Algorithm 2 was run using as initial image estimates bilinearly interpolated images, and the values $\alpha^{c\,(0)} = 0.01$, $\beta^{c\,(0)} = 1000.0$ and $\gamma_{uv}^{cc\prime\,(0)} = 2.0$ (for all $uv \in \mathcal{HB}$ and $c' \neq c$) for all $c \in \{R, G, B\}$. The convergence criterion utilized was $\frac{\|\mathbf{f}^c(k+1)-\mathbf{f}^c(k)\|^2}{\|\mathbf{f}^c(k)\|^2} \leq 10^{-7}$.

Table 1 compares the results obtained by bilinear interpolation, the methods proposed by Laroche [12], Kimmel [11], Gunturk [9] and Algorithm 2. Their performance were evaluated by measuring the SNR improvement in dB, given by

$$\Delta_{SNR} = 10 \times \log_{10}\left[\| \mathbf{f}^c - \mathbf{g}^{\mathrm{pad}\,c} \|^2 \,/\, \| \mathbf{f}^c - \hat{\mathbf{f}}^c \|^2\right],$$

for $c \in \{R, G, B\}$, where $\mathbf{f}^c$ and $\hat{\mathbf{f}}^c$ are the original and estimated high resolution images, and $\mathbf{g}^{\mathrm{pad}\,c}$ is the result of padding missing values at $\mathbf{g}^{\mathrm{obs}\,c}$ (equation 3) with zeroes. Figure 5 shows an enlargement of a small region of the restorations of the image in Figure 4(c) by the different methods under comparison.

a b c

Fig. 4. Images used in the experiments

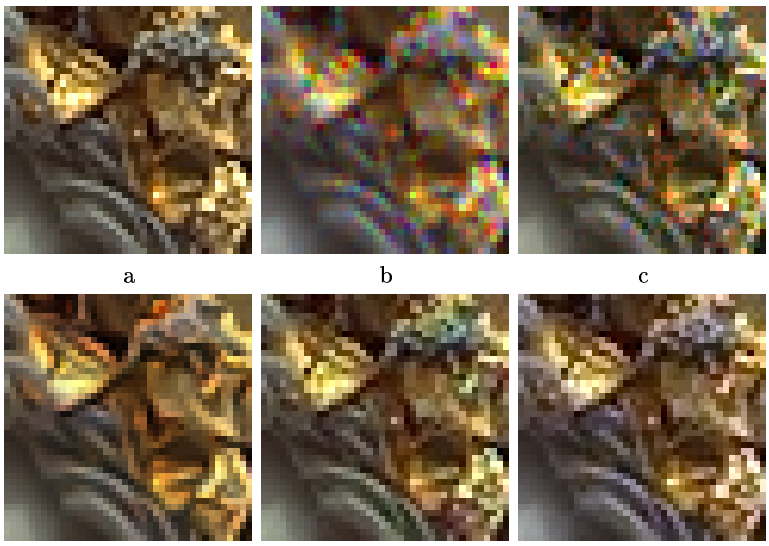

a b c

d e f

Fig. 5. Details of the (a) original image , (b) bilinear reconstruction, (c) Methods of Laroche [12], (d) Kimmel [11], (e) Gunturk [9] and (f) our method.

Table 1. Δ_{SNR} (dB)

image	bilinear			Laroche [12]			Kimmel [11]			Gunturk [9]			our method		
	R	G	B	R	G	B	R	G	B	R	G	B	R	G	B
Fig. 4.(a)	21.0	24.0	20.8	23.1	26.6	27.1	28.2	29.5	28.3	30.3	32.7	29.0	28.4	31.0	29.0
Fig. 4.(b)	20.3	21.7	17.6	18.5	23.9	21.9	26.2	25.5	23.0	27.8	29.5	25.9	29.0	28.6	23.6
Fig. 4.(c)	18.9	19.9	17.6	20.9	21.2	22.2	25.3	24.6	22.6	28.4	30.2	23.6	27.2	28.8	26.7

5 Conclusions

In this paper the color demosaicing problem has been formulated from a super-resolution point of view. A new method for estimating both the reconstructed color images and the model parameters, within the Bayesian framework, was obtained. Based on the presented experimental results, the new method outperforms bilinear interpolation and the methods in [11] and [12], while it performs comparably to the method in [9].

References

1. Bayer, B.E.: Color imaging array (1976) United State Patent 3,971,065.
2. Ramanath, R.: Interpolation Methods for the Bayer Color Array. PhD thesis, North Carolina State University (2000)
3. Alvarez, L., Molina, R., Katsaggelos, A.: High resolution images from a sequence of low resolution observations. In Reed, T.R., ed.: Digital Image Sequence Processing, Compression and Analysis. CRC Press (2004) 233–259
4. Mateos, J., Molina, R., Katsaggelos, A.: Bayesian high resolution image reconstruction with incomplete multisensor low resolution systems. In: 2003 IEEE International Conference on Acoustic, Speech and Signal Processing (ICASSP2003). Volume III., Hong Kong (2003) 705–708
5. Molina, R., Vega, M., Abad, J., Katsaggelos, A.: Parameter estimation in Bayesian high-resolution image reconstruction with multisensors. IEEE Transactions on Image Processing **12** (2003) 1655–1667
6. Katsaggelos, A.K., Lay, K.T., Galatsanos, N.P.: A general framework for frequency domain multi-channel signal processing. IEEE Trans. Image Processing, **2** (1993) 417–420
7. Mateos, J., Vega, M., Molina, R., Katsaggelos, A.: Bayesian image estimation from an incomplete set of blurred, undersampled low resolution images. In: 1st Iberian Conference on Pattern Recognition and Image Analysis (IbPRIA2003), Lecture Notes in Computer Science. Volume 2652. (2003) 445–452
8. Molina, R., Mateos, J., Katsaggelos, A., Vega, M.: Bayesian multichannel image restoration using compound gauss-markov random fields. IEEE Transactions on Image Processing **12** (2003) 1642– 1654
9. Gunturk, B.K., Altunbasak, Y., Mersereau, R.: Color plane interpolation using alternating projections. IEEE Trans. Image Processing, **11** (2002) 997 –1013
10. Molina, R., Katsaggelos, A.K., Mateos, J.: Bayesian and regularization methods for hyperparameter estimation in image restoration. IEEE Trans. Image Processing **8** (1999) 231–246
11. Kimmel, R.: Demosaicing: Image reconstruction from color ccd samples. IEEE Trans. on Image Processing **8** (1999) 1221
12. Laroche, C.A., Prescott, M.A.: Apparatus and method for adaptively interpolating a full color image utilizing chrominance gradients (1994) United State Patent 5,373,322.